Differential localization and identification of a critical aspartate suggest non-redundant proteolytic functions of the presenilin homologues SPPL2b and SPPL3

Peter Krawitz, Christof Haffner, Regina Fluhrer, Harald Steiner, Bettina Schmid, Christian Haass

Angaben zur Veröffentlichung / Publication details:

Krawitz, Peter, Christof Haffner, Regina Fluhrer, Harald Steiner, Bettina Schmid, and Christian Haass. 2005. "Differential localization and identification of a critical aspartate suggest non-redundant proteolytic functions of the presenilin homologues SPPL2b and SPPL3." *Journal of Biological Chemistry* 280 (47): 39515–23. https://doi.org/10.1074/jbc.m501645200.

THE JOURNAL OF BIOLOGICAL CHEMISTRY VOL. 280, NO. 47, pp. 39515–39523, November 25, 2005

Differential Localization and Identification of a Critical Aspartate Suggest Non-redundant Proteolytic Functions of the Presenilin Homologues SPPL2b and SPPL3*

Received for publication, February 11, 2005, and in revised form, April 6, 2005 Published, JBC Papers in Press, July 5, 2005, DOI 10.1074/jbc.M501645200

Peter Krawitz[1], Christof Haffner[1], Regina Fluhrer[1], Harald Steiner, Bettina Schmid[2], and Christian Haass[3]

From the Adolf-Butenandt-Institute, Department of Biochemistry, Laboratory for Alzheimer's and Parkinson's Disease Research, Ludwig-Maximilians-University, Schillerstrasse 44, 80336 Munich, Germany

Signal peptide peptidase (SPP) is an unusual aspartyl protease that mediates clearance of signal peptides by proteolysis within the endoplasmic reticulum (ER). Like presenilins, which provide the proteolytically active subunit of the γ-secretase complex, SPP contains a critical G*X*GD motif in its C-terminal catalytic center. Although SPP is known to be an aspartyl protease of the G*X*GD type, several presenilin homologues/SPP-like proteins (PSHs/SPPL) of unknown function have been identified by data base searches. We now investigated the subcellular localization and a putative proteolytic activity of PSHs/SPPLs in cultured cells and in an *in vivo* model. We demonstrate that SPPL2b is targeted through the secretory pathway to endosomes/lysosomes, whereas SPP and SPPL3 are restricted to the ER. As suggested by the differential subcellular localization of SPPL2b compared with SPP and SPPL3, we found distinct phenotypes upon antisense gripNA-mediated knockdown in zebrafish. *spp* and *sppl3* knockdowns in zebrafish result in cell death within the central nervous system, whereas reduction of *sppl2b* expression causes erythrocyte accumulation in an enlarged caudal vein. Moreover, expression of D/A mutations of the putative C-terminal active sites of *spp*, *sppl2*, and *sppl3* produced phenocopies of the respective knockdown phenotypes. Thus, our data suggest that all investigated PSHs/SPPLs are members of the novel family of G*X*GD aspartyl proteases. Furthermore, SPPL2b is shown to be the first member of the SPP/PSH/SPPL family that is not located within the ER but in endosomal/lysosomal vesicles.

Intramembrane proteolysis is mediated by a class of novel polytopic proteases that have their active centers located within the hydrophobic transmembrane domains (1, 2). Members of these proteases include the site-two protease (1), rhomboids (3, 4), γ-secretase (5), and signal peptide peptidase (SPP)[4] (6, 7). Although the site-two protease and rhomboids belong to the class of metallo- and serine proteases, respectively, γ-secretase and SPP are aspartyl proteases (2, 8, 9). Intramembrane-cleaving cysteine proteases have so far not been identified. It should, however, be noted that the precise cleavage sites of the site-two protease, rhomboids, and SPPs have not yet been directly determined; thus, it remains possible that cleavage could also occur at or close to the membrane.

The catalytic core of γ-secretase is provided by either of the two homologous presenilins (PS1 or PS2). Co-factors including anterior pharynx defective 1 (APH-1), presenilin enhancer (PEN)-1, PEN-2, and Nicastrin are absolutely required to generate a functional γ-secretase complex (10–14). PS1- or PS2-containing γ-secretase complexes can both mediate the intramembrane cleavage of the β-amyloid precursor protein (APP), Notch, and probably many other type I-oriented substrates as well (8, 15–18), suggesting functional redundancy. Moreover, several distinct species of APH-1 also appear to be functionally redundant at least with respect to γ-secretase-mediated cleavage of β-amyloid precursor protein fragments (19, 20). However, recent evidence (21) suggests that γ-secretase complexes containing different APH-1 species may have tissue-specific activities. In addition, differential activities of individual complexes within different subcellular compartments can also not be excluded.

The C-terminal critical aspartate of PSs is located within a conserved G*X*GD motif (22), whereas the N-terminal aspartate is embedded within a YD sequence segment. The G*X*GD signature motif is highly conserved in SPP, an unrelated polytopic aspartyl protease (2, 7, 23, 24), as well as in the type four prepilin peptidases (22, 25). Moreover, mutagenesis of the corresponding aspartate residue blocks the proteolytic activity of SPP (7), PS1 (5), PS2 (15, 26), and type four prepilin peptidases (25). This strongly suggests that the aspartate within the G*X*GD motif comprises the C-terminal active site of these proteases. Furthermore, SPP can also be targeted with highly specific γ-secretase inhibitors, demonstrating the similarity of the catalytic centers of SPP and γ-secretase (27–29). Further similarities are observed between PSs, SPP, and type four prepilin peptidases, which also include a P*X*L motif within the C-terminal domain. SPP is required for the removal of signal peptides (2). In addition, SPP is also involved in immune surveillance and processing of the hepatitis C viral core protein (7), suggesting a more general role of SPP in the liberation of bioactive peptides (2, 7, 23, 24). Besides SPP, a family of homologous proteins was identified by data base searches (2, 7, 23, 30, 31). These proteins were named SPPL (SPP-like) 2 (a, b, c) and 3 (in yeast an additional SPPL, SPPL4, exists) (7) or PS homologues 1–5 (30). For clarity, we will use the term SPPL throughout this manuscript. Although SPPLs share some homology with SPPs, it is not known if they exhibit any proteolytic activity (24).

We now investigated the subcellular distribution and catalytic function of SPP and SPPLs in human cells and in zebrafish and suggest that

* This work was supported by the Deutsche Forschungsgemeinschaft (the DFG Priority program "Cellular Mechanisms of Alzheimer Disease" (to C. Haass, H. Steiner, and C. Haffner) and SFB 596 "Molecular Mechanisms of Neurodegeneration" (to C. Haass and B. Schmid), the Leibniz Award (to C. Haass), the APOPIS Program funded by the European Union under the Sixth Framework Programme; Contract LSHM-CT-2003-503330 (to C. Haass), and the Molecular Medicine Program of the Ludwig-Maximilians-University (FöFoLe) (to P. Krawitz). The costs of publication of this article were defrayed in part by the payment of page charges. This article must therefore be hereby marked "*advertisement*" in accordance with 18 U.S.C. Section 1734 solely to indicate this fact.

The nucleotide sequence(s) reported in this paper has been submitted to the GenBank™/EBI Data Bank with accession number(s)AY926458 (spp), AY926457 (sppl2) and AY926459 (sppl3).

[1] These authors contributed equally.

[2] To whom correspondence may be addressed. Tel.: 49-89-2180-75453; Fax: 49-89-2180-75415; E-mail: beschmid@med.uni-muenchen.de.

[3] To whom correspondence may be addressed. Tel.: 49-89-2180-75471; Fax: 49-2180-75415; E-mail: Christian.Haass@med.uni-muenchen.de.

[4] The abbreviations used are: SPP, signal peptide peptidase; SPPL, SPP-like proteins; PS, presenilin; APP, β-amyloid precursor protein.

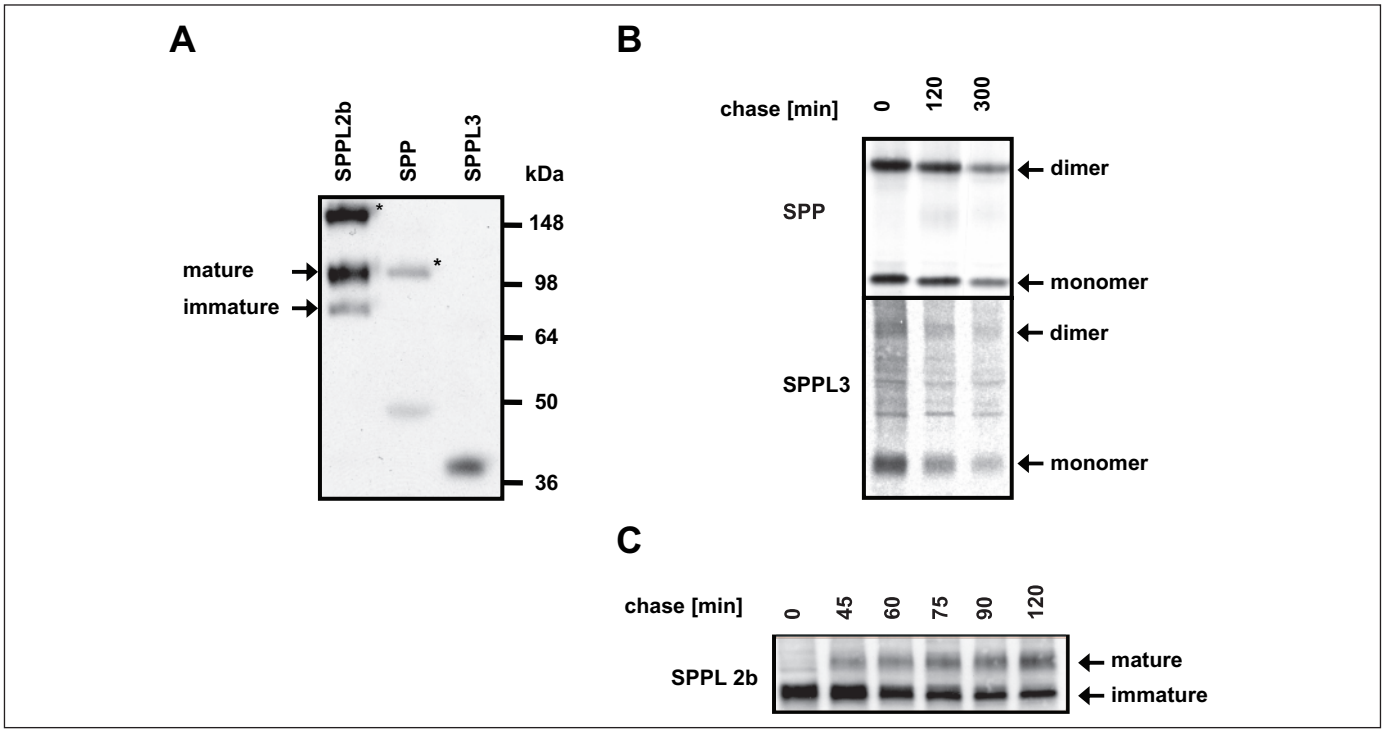

FIGURE 1. **Expression and maturation of SPP and SPPLs.** *A*, lysates of HEK293 cells stably transfected with Myc-tagged SPPL2b (*lane 1*), SPP (*lane 2*), or SPPL3 (*lane 3*) were immunoprecipitated with antibodies N159, 2812, or 4a, respectively. Immunoprecipitated SPP or SPPLs were identified with the anti-Myc antibody 9E10. Mature and immature forms of SPPL2b are indicated by *arrows*. Bands marked with an *asterisk* (*) represent the putative dimeric forms of the respective protein. Note that tags do not affect expression and membrane orientation of SPP/SPPL (38). *B*, HEK293 cells stably expressing SPP and SPPL3 were pulse-labeled with [^{35}S]methionine/cysteine for 15 min and chased for the time points indicated. Proteins were immunoprecipitated using the 9E10 antibody and detected by autoradiography. Note that neither SPP nor SPPL3 undergoes a molecular weight shift during the chase period. *C*, HEK293 cells stably expressing SPPL2b were pulse-labeled with [^{35}S]methionine/cysteine for 15 min and chased for the time points indicated. Proteins were immunoprecipitated using the 9E10 antibody and detected by autoradiography. Note that SPPL2b undergoes a molecular weight shift during the chase period.

SPPLs are novel members of the family of aspartyl proteases of the G*X*GD type. Moreover, by demonstrating an endosomal/lysosomal localization of SPPL2b, we provide first evidence that the function of these proteases may not be necessarily restricted to the ER and the removal of signal peptides within the early secretory pathway.

EXPERIMENTAL PROCEDURES

Cell Culture, cDNAs, and Transfection—HEK293 cells were cultured in Dulbecco's modified Eagle's medium with Glutamax (Invitrogen) supplemented with 10% fetal calf serum (Invitrogen). SPP, SPPL2b, and SPPL3 cDNAs were amplified by PCR from a human brain cDNA library using the following primers: SPP, 5′-CGCGAATTCGCCACCATGGACTCGGCCCTCAGC-3′ and 5′-CGCCTCGAGTTTCTCTTTCTTCTCCAGCC-3′; SPPL2b, 5′-CGCGAATTCGCCACCATGGCGGCAGCGGTGGCGGCTG-3′ and 5′-CGCCTCGAGCTAGGCCGAGGCGCCAGGCTGG-3′; SPPL3, 5′-CGCGAATTCGCCACCATGGCGGAGCAGACCTACTCGT-3′ and 5′-CGCCTCGAGTACTTCCAGGAATCGGGAGCTG-3′.

SPP and SPPL3 were subcloned into the pcDNA4/TO/Myc-His vector and transfected into HEK293 TR cells (Invitrogen). SPPL2b was subcloned into pcDNA4/Myc-His (Invitrogen) and transfected into a HEK293 cell line stably overexpressing APP 695 containing the Swedish mutation (32, 33). Transfection of cells was carried out using Lipofectamine 2000 (Invitrogen) according to the supplier's instructions, and single cell clones were generated by selection in 200 μg/ml zeocin (Invitrogen). To induce expression of SPP and SPPL3, cells were incubated with 1 μg/ml doxycycline added to the cell culture medium for 48 h.

Antibodies, Metabolic Labeling, Immunoprecipitation, and Immunoblotting—The polyclonal anti-SPP antibody 2812 (against amino acids 201–377 of human SPP) and polyclonal anti-SPPL3 antibody 4a (against amino acids 370–384 of human SPPL3) were obtained from Memorec Biotech GmbH (Cologne). The polyclonal anti-SPPL2b antibody N159 was generated by immunization of rabbits with a synthetic peptide representing the amino acids 213–227 of human SPPL2b coupled to keyhole limpet hemocyanin (Eurogentec, Seraing, Belgium). The monoclonal anti-Myc antibody 9E10 and the monoclonal anti-LAMP2 antibody were obtained from the hybridoma bank, the monoclonal anti-BiP antibody was from Stressgen, and the polyclonal anti-calreticulin antibody was from Calbiochem. Pulse-chase experiments, cell lysis, and immunodetection were carried out as described before (34).

Deglycosylation Experiments—For the deglycosylation experiments cell lysates were denatured with 1% SDS for 10 min at 65 °C, diluted 1:10 in assay buffer (50 mM sodium phosphate, pH 7.2, 12 mM EDTA, 0.4% Nonidet-P40) to a protein concentration of ~ 1 μg/μl, and treated overnight at 37 °C with 50 milliunits/ml *N*-glycosidase F (Roche Applied Science) or 0.25 milliunits/μl endoglycosidase H (Roche Applied Science).

Immunofluorescence Microscopy—Cells were grown on polylysine-coated coverslips, fixed for 20 min with phosphate-buffered saline (PBS), 3.7% paraformaldehyde, permeabilized for 20 min with PBS, 0.2% Triton X-100, and blocked with PBS, 1% bovine serum albumin. Antibody incubations were performed for 1 h at room temperature in phosphate-buffered saline followed by incubation with Alexa 488- and Alexa 594-coupled secondary antibodies (Molecular Probes), and mounted samples were analyzed with a Zeiss Axioplan fluorescent microscope.

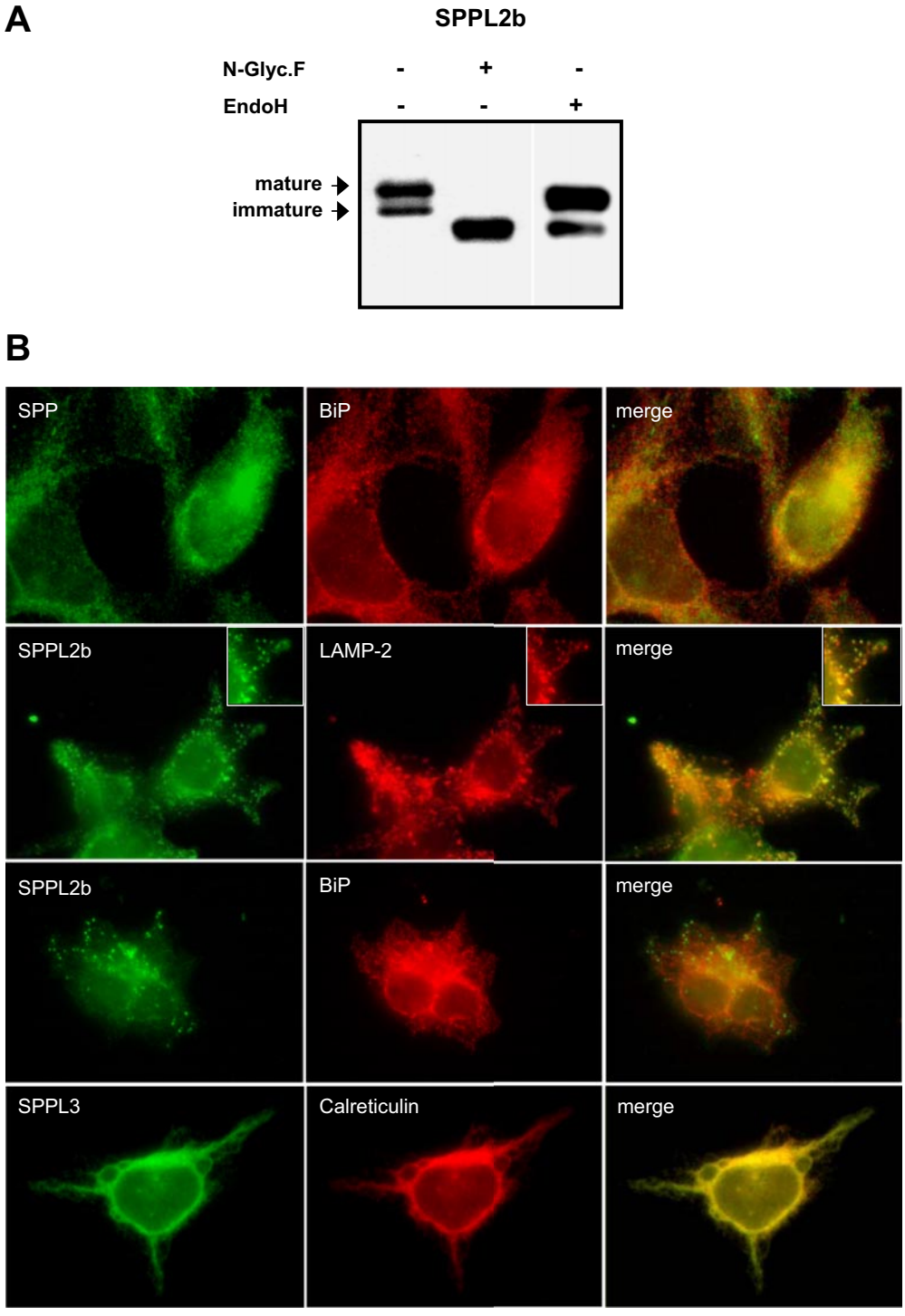

FIGURE 2. **Posttranslational maturation and endosomal localization of SPPL2b.** *A*, SPPL2b is a glycoprotein that undergoes complex glycosylation. Protein extracts of HEK293 cells stably transfected with SPPL2b were treated with *N*-glycosidase F (*N-Glyc.F*) or endoglycosidase H (*EndoH*). SPPL2b was detected with the anti-Myc antibody 9E10. In untreated extracts monomeric SPPL2b appears as two bands of 90 and 110 kDa. Whereas treatment with *N*-glycosidase F shifts both bands completely to a single band of 65 kDa, treatment with endoglycosidase H causes only a very minor shift of the upper band, suggesting that this species is partially endoglycosidase H-resistant. *B*, subcellular localization of SPP and SPPLs. Immunofluorescence microscopy reveals that SPP and SPPL3 colocalize to a large extent with the ER-resident proteins BiP and calreticulin. In contrast, SPPL2b staining shows significant overlap with LAMP-2, a marker for late endosomes/lysosomes, whereas very little co-localization is observed with BiP. *Insets* show extensive co-localization of SPPL2b with LAMP-2-positive vesicles.

Fish Maintenance and Breeding—Zebrafish were maintained, mated, and raised as described (35). Embryos were kept at 28 °C and staged as described (36). The wild type line AB was used for all experiments.

In Situ Hybridization and Acridine Orange Staining—*In situ* hybridizations were carried out as described elsewhere (37) with slight modifications. The single-stranded RNA probes were labeled with digoxigenin-UTP (Roche Applied Science). The second antibody was preincubated overnight with zebrafish embryos. All washing steps were carried out at 65 °C. Washes were as follows: 2× 30 min in 50% formamide, 2× SSCT (standard saline critrate + 0.1% Tween); 1× 15 min in

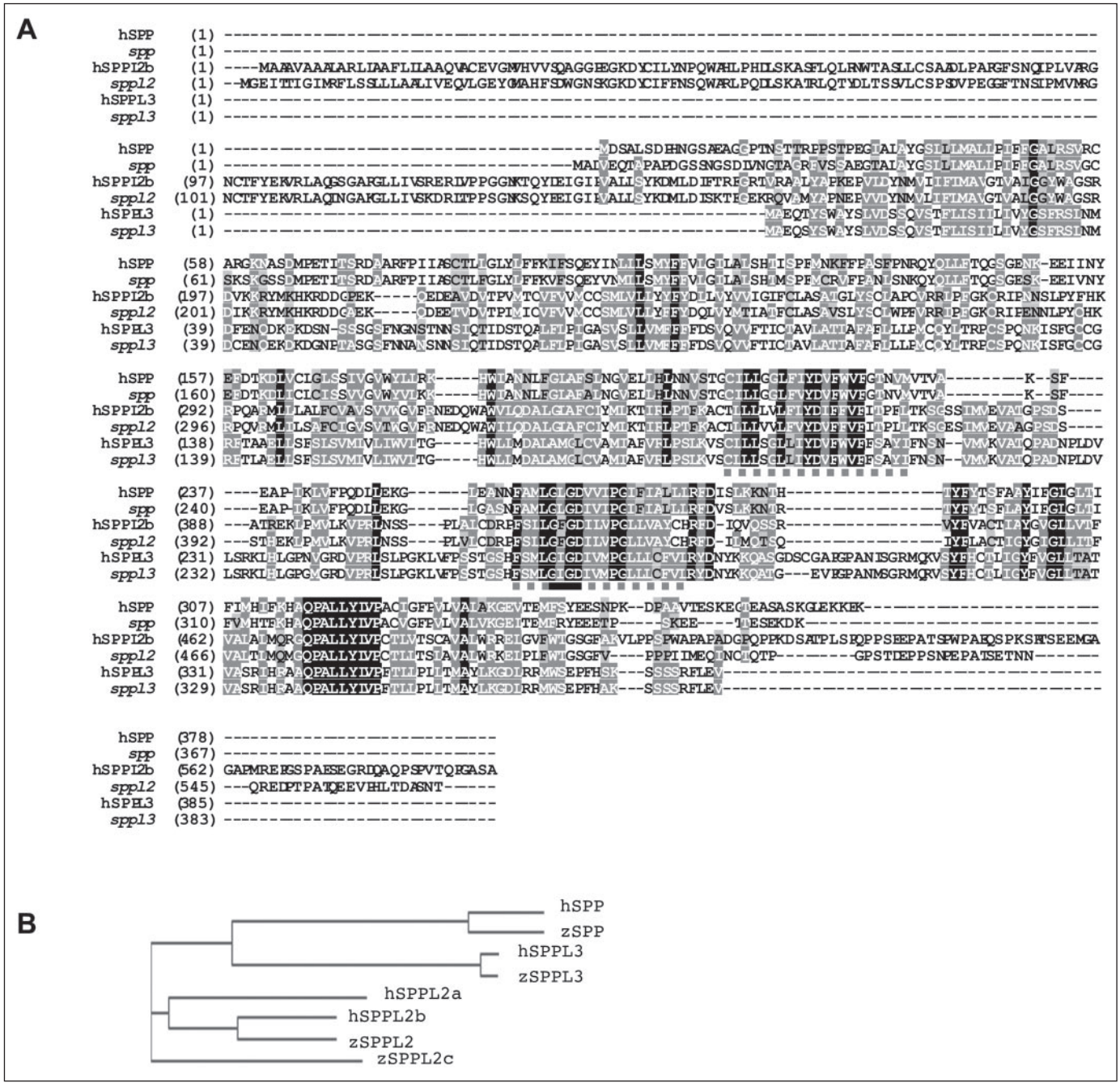

FIGURE 3. **Amino acid sequence alignment of members of the SPP family.** *A*, amino acid sequence alignment of human (*h-*) SPP/SPPLs and their zebrafish homologues. *Black shading* indicates complete conservation in all proteins, and *gray shading* indicates biochemically similar residues. *Dotted lines* highlight the predicted active site transmembrane domains, and the *bar* highlights the G*X*GD motif. *B*, phylogenetic tree based on the neighbor joining algorithm showing the evolutionary distances.

2× SSCT; 2× 30 min in 0.2× SSCT. To reduce endogenous phosphatase activity, 0.25 mg/ml levamisole was added to the staining buffer. Dechorionated embryos were incubated alive in 2 mg/ml acridine orange in E3 medium for 30 min at room temperature. Stained embryos were analyzed after 3 wash steps of 5 min with E3 medium.

Antisense gripNAs and Microinjection of Zebrafish Embryos—Antisense gripNAs of 18 nucleotides in length were obtained from Active Motif. For *spp* and the *sppl* genes we used a grip designed against the ATG-start codon (ATG-grip) to block translational start (the ATG site is in bold) and an independent gripNA hybridizing to an exon-intron junction, resulting in a nonsense splicing product (GT-grip). As controls, three bases of the ATG-grip were modified (underlined below). In the case of *spp* the ATG control grip is shifted five nucleotides further upstream in addition to the two modified nucleotides: spp ATG-grip, 5′-CTGCTCCACATCCGC**CAT**-3′; spp GT-grip, 5′-CGTACCTCATTGTGTGAG-3′; spp ATG-control grip, 5′-CTACATTCGC**CAT**GCTTC-3′; sppl2 ATG-grip, 5′-TGTGATCTCCC**CAT**CCG-3′; sppl2 GT-grip, 5′-CTTACTTTTTCCTGTCCC-3′; sppl2 ATG-control grip, 5′-TATGATCTCGC**CAT**ACG-3′; sppl3 ATG-grip, 5′-CTCTGCTCCGC**CAT**GTCA-3′; sppl3 GT-grip, 5′-CGCACCGTCCATGAGCAG-3′; sppl3 ATG-control grip, 5′-CTCGGCTCCGCAATGCCA-3′.

Embryos were microinjected with a Femto Jet Microinjector (Eppendorf) at the one-cell stage with gripNA concentrations varying from 0.12 to 1.0 mM depending on the severity of the observed phenotype.

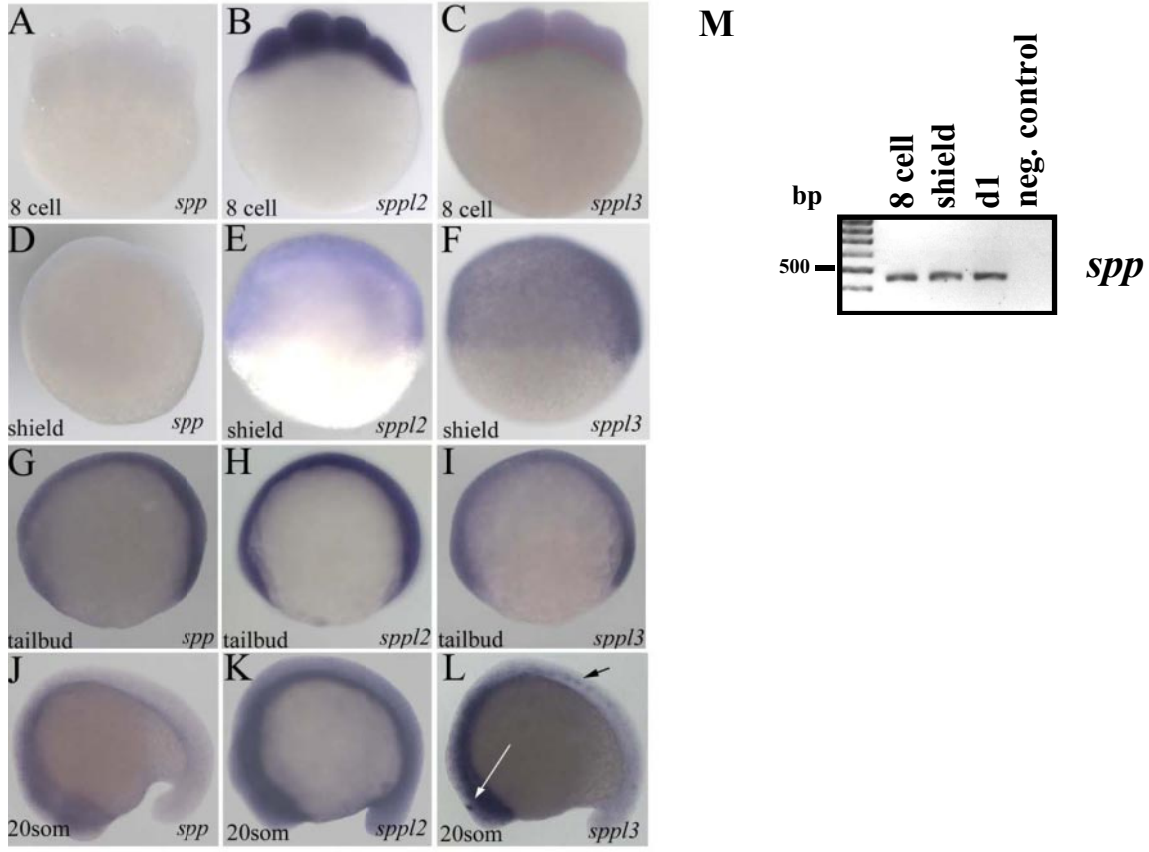

FIGURE 4. **Expression profiles of *spp*, *sppl2*, and *sppl3* during early zebrafish development and somitogenesis revealed by whole mount *in situ* hybridization.** Ubiquitous expression of *sppl2* and *sppl3* at the eight-cell and shield stage is observed (*B*, *C*, *E*, and *F*). *spp*, although maternally inherited (as detected by reverse transcription-PCR; *M*), is not detectable in these stages by *in situ* hybridization (*A* and *D*). Ubiquitous expression of all three genes at the tail-bud stage (*G*, *H*, and *I*). At the 20-somite stage expression of *spp* and *sppl3* becomes largely restricted to the central nervous system (*J* and *L*), whereas *sppl2* expression remains ubiquitous (*K*). *L*, the additional signal of *sppl3* transcripts in the epiphysis (*white arrow*) and somites (*som*) (*black arrow*). *M*, analysis of early expression of *spp* by reverse transcription-PCR. *d1*, day 1; *neg. control*, negative control. Embryos are shown in lateral view; *D–I*, ventral to the *left*; *J–L*, anterior to the *left*.

The injected volume was 2–4 pl. After injection the embryos were maintained in embryo medium at 28 °C.

Zebrafish cDNA Constructs, mRNA Synthesis, and Generation of Mutant mRNA—cDNA clones encoding *spp* (MPMGp637A0723Q2), *sppl2* (MPMGp609O0125Q8), and *sppl3* (MPMGp637N1021Q2) were obtained from the German Resource Centre for Genome Research (RZPD) (www.rzpd.de). Sequences were submitted to GenBank™ (accession numbers are AY926458 for *spp*, AY926457 for *sppl2* and AY926459 for *sppl3*). Full-length *spp*, *sppl2*, and *sppl3* were subcloned into the pCS2+ (sitemaker.umich.edu/dlturner.vectors) expression vector. mRNA was synthesized using the mMESSAGE MACHINE kit (Ambion) and polyadenylated using a polyadenylation kit (Ambion) according to the manufacturer's instructions. The codon encoding the critical aspartate was mutagenized to an alanine codon after the QuikChange (Stratagene) protocol. Successful mutagenesis was verified by DNA sequencing.

RESULTS

Differential Subcellular Localization of SPPLs—Besides SPP itself, the SPP family comprises four additional members of unknown function in mammals, two of which, SPPL2b and SPPL3, are conserved in all vertebrates ((7, 30); see also Fig. 3). They were, therefore, chosen for a functional analysis in cultured cells and in zebrafish as a model system. As a first step we examined expression and maturation of Myc-tagged human SPPL2b (the only SPPL2 present in the zebrafish genome; see Fig. 3) and SPPL3 in comparison to SPP in HEK293 cells. Clones stably expressing SPP/SPPLs were generated, and expression levels were analyzed (Fig. 1*A*). As shown previously, two major SPP bands were detected, which may represent monomeric and dimeric variants (28, 38). SPPL2b was expressed as two bands of 90 and 110 kDa (Fig. 1*A*), molecular masses considerably higher than predicted (64.7 kDa). In addition, a higher molecular mass band was also observed, again suggesting oligomerization to a variable degree (Fig. 1*A* (38)). SPPL3 was observed as an ~40-kDa protein (Fig. 1*A*). As for SPP and SPPL2b, dimers and higher molecular mass oligomers of SPPL3 were sometimes observed (see also Fig. 1*B*; *lower panel*).

To investigate whether the two immunoreactive bands of SPPL2b result from posttranslational modification, pulse-chase experiments were performed. Whereas SPP and SPPL3 showed no posttranslational maturation (as monitored by the absence of a molecular mass shift during the chase period; Fig. 1*B*), SPPL2b is expressed at time point 0 min as a single band, which during the chase period is reduced at the expense of a higher molecular mass protein (Fig. 1*C*). This may suggest that SPPL2b posttranslationally maturates by glycosylation during its targeting through the secretory pathway. Putative glycosylation of SPPL2b was, therefore, further investigated by selective removal of *N*-linked sugar side chains (Fig. 2*A*). *N*-Glycosidase F treatment of cell lysates from SPPL2b-expressing cells resulted in the detection of a single band of ~70 kDa, which roughly corresponds to the calculated molecular mass of SPPL2b (64.7 kDa). In contrast, endoglycosidase H treat-

TABLE ONE

Phenotypic effects of knockdown and loss-of-function variants of spp/*sppl*

p value is derived from χ^2 test against the control group, wt, wild type.

spp	Concentration	*n*	Neuronal degeneration	No phenotype	Unspecific	*p*
			%	%	%	
spp ATG-grip	0.12 mM	97	85	14	1	0.0001
spp GT-grip	1 mM	117	70	28	2	0.0001
spp ATG-control grip	1 mM	47	0	94	6	
spp D268A capped mRNA	0.75 μM	110	26	66	7	0.0193
spp wt capped mRNA	1 μM	39	5	85	10	
sppl2	**Concentration**	***n***	**Blood clot**	**No phenotype**	**Unspecific**	***p***
			%	%	%	
sppl2 ATG-grip	1 mM	188	76	22	4	0.0001
sppl2 GT-grip	1 mM	205	86	10	4	0.0001
sppl2 ATG-control grip	1 mM	121	4	95	1	
sppl2 GT-grip	0.75 mM	142	86	8	5	
sppl2 GT-grip + *sppl2* wt mRNA	0.75 mM + 0.36 μM	119	41	54	5	0.0001
sppl2 D422A mRNA	0.36 μM	123	49	43	8	0.0001
sppl2 wt mRNA	0.36 μM	49	0	96	4	
sppl3	**Concentration**	***n***	**Neuronal degeneration**	**No phenotype**	**Unspecific**	***p***
			%	%	%	
sppl3 ATG-grip	0.5 mM	269	84	14	2	0.0001
sppl3 GT-grip	0.5 mM	148	70	27	3	0.0001
sppl3 ATG-control grip	0.5 mM	53	0	96	4	
sppl3 D272A mRNA	0.63 μM	159	48	45	7	0.0001
sppl3 wt mRNA	0.63 μM	31	0	94	6	

ment caused only a minor shift of the upper band to a lower molecular mass (Fig. 2*A*), whereas the lower molecular weight variant of SPPL2b was fully endoglycosidase H-sensitive (Fig. 2*A*). This demonstrates that the upper band of SPPL2b becomes partially endoglycosidase H-resistant (as observed for example for nicastrin (39–41)) and strongly suggests passage through the Golgi apparatus. This is somewhat surprising since proteins of the SPP family may have been expected to be located within early secretory compartments, namely the ER, where signal peptide cleavage occurs (7, 42). Accordingly, SPP even appears to be actively retained within the ER by a KK*XX* ER retrieval signal (7).

To further substantiate trafficking of SPPL2b through the secretory pathway, an indirect immunofluorescence analysis was performed. As expected (7) SPP co-localized with the ER marker BiP (Fig. 2*B*). In cells overexpressing SPPL3, a similar staining pattern was observed that again overlapped with an ER marker (Fig. 2*B*), suggesting that SPPL3 also localizes to the ER. In contrast, SPPL2b was found predominantly in vesicular structures, which were positive for LAMP-2 (Fig. 2*B*), a marker for late endosomes/lysosomes (43). Co-staining with the ER marker BiP showed little co-localization, demonstrating that SPPL2b does not accumulate within the ER (Fig. 2*B*). The small amounts of SPPL2b found in the ER may be due to immature SPPL2b transported through the early secretory pathway. Thus, the data from indirect immunofluorescence are consistent with our observation from the pulse-chase and deglycosylation experiments (Figs. 1, *B* and *C* and 2*A*) and demonstrate that SPPL2b, in contrast to SPP and SPPL3, is targeted through the entire secretory pathway to endosomes/lysosomes. These data demonstrate that not all proteins of the SPP family are restricted to the early secretory compartment, indicating functional diversity.

Identification and Developmental Expression of Zebrafish SPPLs—To investigate putative individual proteolytic functions of SPPLs *in vivo*, we turned to zebrafish as a model system. We have used this system previously to study γ-secretase function *in vivo* and to elucidate the function of the Nicastrin-like protein Nicalin (44–46). Sequence comparison of zebrafish *spp* and *sppl*s revealed a significant homology to the human counterparts (Fig. 3*A*). Interestingly, we found only one *sppl2* homologue within the zebrafish genome, which shares highest sequence identity with SPPL2b (66% compared with 50% with SPPL2a and 45% with SPPL2c (Fig. 3, *A* and *B*)). We refer to this gene as *sppl2* for the remainder of the manuscript (according to the Zebrafish Nomenclature Committee).

To gain first insight into *spp* and *sppl* function, we visualized mRNA localization by whole mount *in situ* hybridization during development. Significant amounts of *sppl2* and *sppl3* mRNAs were detectable before zygotic transcription at the eight-cell stage, revealing maternal inheritance (Fig. 4,*B* and *C*). *sppl2* and *sppl3* are ubiquitously expressed until tail-bud stage (Fig. 4, *H* and *I*). Transcripts of *spp* became first detectable by whole mount *in situ* hybridization at tail-bud stage (Fig. 4*G*). However, we expected *spp* to also be expressed early during development since SPP has been shown to clear signal peptides (7), a process most likely required at all stages of development. Analysis of early stage embryos by a more sensitive reverse transcription-PCR approach revealed the expected maternal inheritance of *spp* and expression at all stages analyzed (Fig. 4*M*). Transcripts of *spp*, *sppl2*, and *sppl3* are ubiquitously expressed at the five-somite stage (data not shown). From the 20-somite stage onward, expression of *spp* and *sppl3* becomes restricted to the central nervous system, whereas *sppl2* appears to be more ubiquitously expressed (Fig. 4, *J–L*). *sppl3* transcripts are additionally detected in the epiphysis and in somites at the 20-somite stage (Fig. 4*L*). All *spp* and *sppl* transcripts are continuously expressed throughout the brain from day 1 until day 3 post-fertilization (data not shown).

Knockdown of Zebrafish spp and sppl—To gain further insight into the *in vivo* function of *spp* family members, we transiently knocked

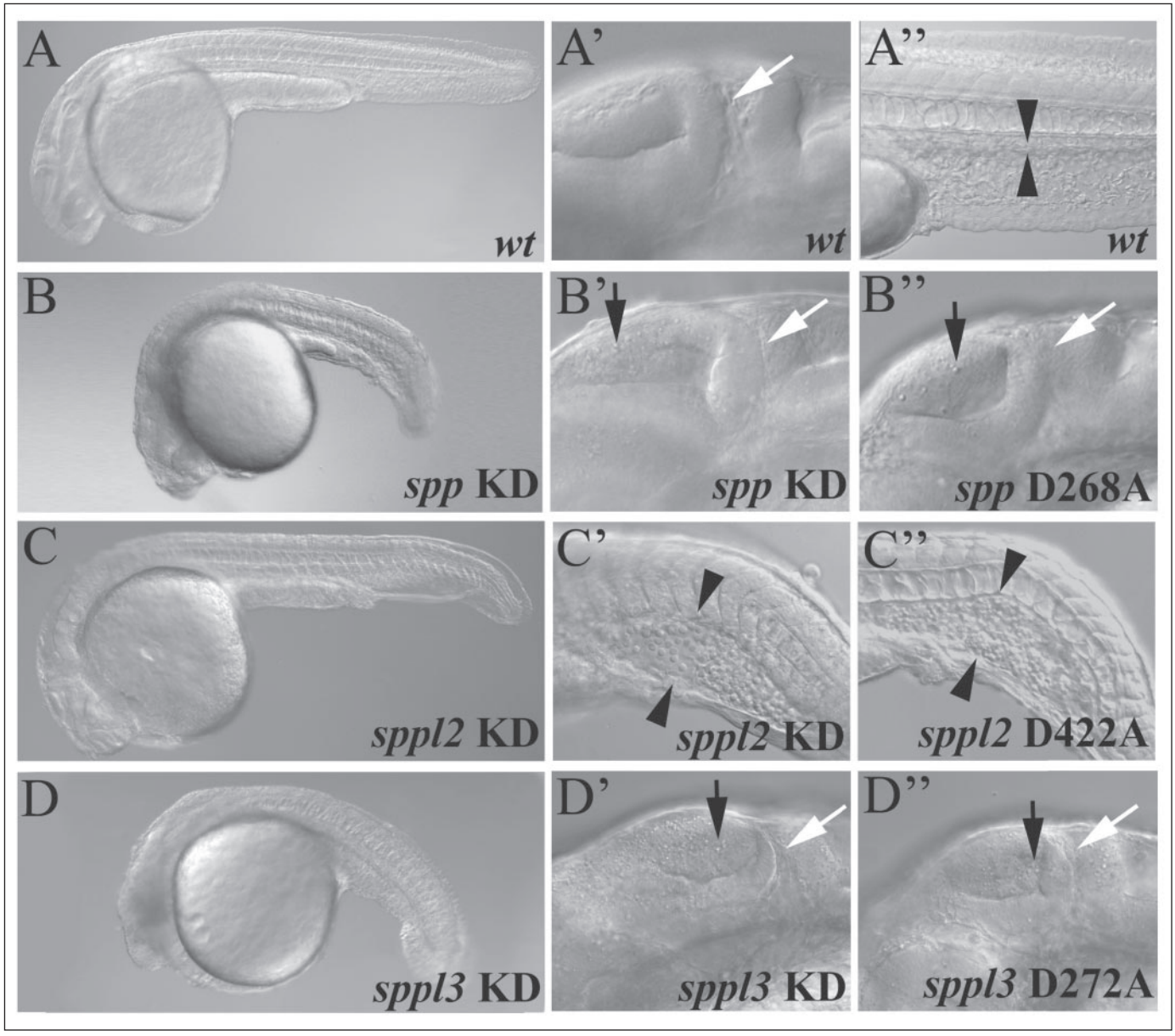

FIGURE 5. **Loss-of-function phenotypes of *spp* and *sppl* in zebrafish.** Uninjected embryo at 24 h post-fertilization (*A*) showing the normal midbrain-hindbrain boundary (*A′*, *white arrow*) and a wild type (*wt*) caudal vein (*A″*, *arrowheads*). Knockdown (*KD*) of *spp* (ATG-grip) results in cell death within the nervous system (*B* and *B′*). Dead cells are visible in the midbrain and are clearly distinguishable by their round morphology (*black arrows* in *B′* and *B″*). Overexpression of *spp* D268A mRNA phenocopies the *spp* knockdown phenotype (*B″*). Embryos injected with *sppl2* ATG-grip show erythrocyte accumulation in the enlarged caudal vein (*arrowheads* in *C′*). Embryos injected with *sppl2* D422A mRNA show the *sppl2* knockdown phenotype (*C″*). Injection of *sppl3* ATG-grip results in broad cell death within the nervous system (*D* and *D′*). Dead cells are present throughout the central nervous system (*black arrows* in *D′* and *D″*). Overexpression of *sppl3* D272 mRNA phenocopies the *sppl3* knockdown phenotype (*D″*). *White arrows* mark the midbrain-hindbrain boundary. All embryos are oriented with anterior to the left and posterior to the right. Higher power views in *B′*, *B″*, *D′*, and *D″* show less severely affected embryos compared with embryos shown in *B* and *D*.

down *spp* and *sppl*s by injection of antisense gripNAs into one-cell stage zebrafish embryos. Injection of a gripNA targeting the start codon of *spp* (referred to as *spp* ATG-grip) led to a cell death phenotype within the nervous system (85% of cases, $n = 97$; TABLE ONE; Fig. 5, *B* and B′). An indistinguishable phenotype was obtained by injection of a *sppl3* ATG-grip (84% of cases, $n = 269$) (Fig. 5, *D* and *D′*). In contrast, knockdown of *sppl2* by injection of a *sppl2* ATG-grip resulted in a distinct phenotype with an enlarged caudal vein accumulating blood (76% of the cases; $n = 188$) (Fig. 5, *C* and *C′*). To rule out defects in endothelial and hematopoietic differentiation, several *in situ* markers were tested (*flt4*, *krox20*, *scl*, *ephB4*, *flk1*, *gata1*). None of these markers revealed differences compared with uninjected control embryos (data not shown).

To demonstrate the cell death phenotype in *spp* and *sppl3* knockdown embryos more directly, we used the cell death marker acridine orange (47). Staining of non-injected embryos did not show cell labeling above background levels (Fig. 6*A*). In contrast, staining of *spp*-grip- and *sppl3*-grip-injected embryos resulted in the massive labeling of cells in the brain and the spinal cord (Fig. 6, *B* and *D*). In both cases we observed a range of phenotypes of different strength. Figs. 5, *B* and *D*, show more strongly affected embryos, demonstrating pronounced cell death. We selected less severely affected embryos for Figs. 5, *B′* and *D′*, and 6 to visualize individual dying cells. Acridine orange staining of *sppl2* knockdown embryos did not result in significant cell labeling, demonstrating the absence of cell death (Fig. 6*C*).

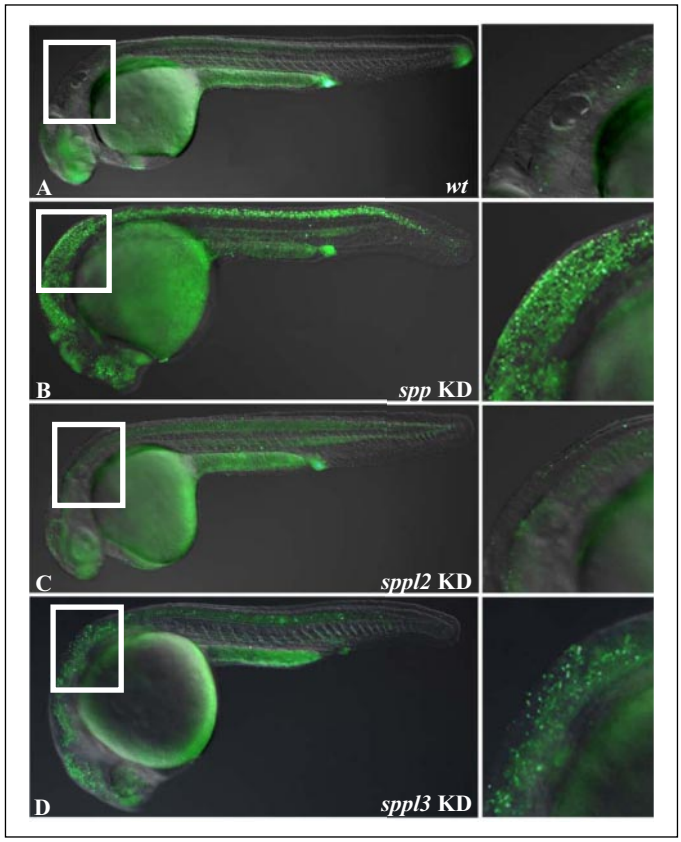

FIGURE 6. **Cell death in *spp* and *sppl3* loss-of-function phenotypes.** Acridine orange stains dying cells. In wild type (*wt*) embryos only a few dying cells are seen at 24 h post-fertilization (*A*). In *spp* knockdown (*KD*) embryos (GT-grip) dead cells are seen evenly distributed throughout the central nervous system and spinal cord (*B*). *sppl2* knockdown embryos (GT-grip) do not show significantly elevated cell death compared with wild type embryos (*C*). *sppl3* knockdown embryos (ATG-grip) show cell death throughout the brain (*D*). The *white rectangles* mark the areas of the higher power magnifications shown on the right. In *B* and *D* less severely affected embryos are shown to allow visualization of individual cells. Autofluorescence of the yolk is observed in *A–D*.

A number of control experiments were performed to demonstrate the specificity of the observed phenotypes. Injection of control gripNAs did not lead to significant defects (TABLE ONE). Moreover, the individual phenotypes were reproduced by injection of independent gripNAs targeting splice donor sites of *spp*, *sppl2*, and *sppl3* transcripts (referred to as GT-grips; TABLE ONE). The *sppl2* GT-grip-induced knockdown phenotype could additionally be rescued by coinjection of wild type *sppl2* mRNA. The percentage of embryos showing a phenotype could be significantly reduced from 86% ($n = 142$) to 41% ($n = 119$) (TABLE ONE), again demonstrating its specificity. Taken together, we have generated knockdown phenotypes of *spp* and *sppl* by two independent gripNAs, targeting the start codons and splice donor sites, revealing distinct phenotypes for *sppl2* and *spp*/*sppl3*.

Overexpression of Dominant Negative Mutants Phenocopies the Knockdown Defects—We next wanted to analyze if the observed *spp* knockdown phenotype can be correlated to its catalytic function. One possibility to examine this is the expression of loss-of-function mutants. Weihofen *et al*. (7) have shown that mutagenesis of the aspartate within the G*X*GD motif (Asp-265 in human SPP) to alanine abolishes proteolytic activity of SPP. We, therefore, generated the corresponding D268A mutation in *spp* and injected the mRNA into one-cell stage embryos. This resulted in a neuronal cell death phenotype very similar to that seen in the *spp* knockdown embryos (Fig. 5, compare *B′* and *B″*; TABLE ONE). Thus, the observed knockdown phenotype is not only specific but is most likely caused by a loss of *spp* activity. Like SPP, all members of the SPPL family contain a G*X*GD motif at the corresponding positions of their transmembrane domains (Fig. 3*A*) and might, therefore, also represent G*X*GD type aspartyl proteases. Analogous to SPP, we therefore mutagenized the corresponding aspartates to alanine and injected the mutant mRNAs into one-cell stage embryos. *sppl2* D422A mRNA injection led to blood clots in 49% of cases ($n = 123$) (Fig. 5, compare *C′* and *C″*), whereas injection of wild type *sppl2* mRNA of the same concentration did not cause any phenotype (TABLE ONE). Similarly, injection of *sppl3* D272A mRNA but not wild type mRNA phenocopied the *sppl3* knockdown phenotype in 48% of the injected embryos ($n = 159$) (Fig. 5, compare *D′* and *D″*) (TABLE ONE). Taken together, these data confirm the corresponding knockdown phenotypes and suggest that *sppl2* and *sppl3* are also likely to function as aspartyl proteases of the G*X*GD type.

DISCUSSION

Upon the identification of SPP, data base searches revealed a family of SPP homologues, the SPPLs/PSHs (7, 30). However, it remained unknown whether these proteins are proteolytically active and whether they are functionally redundant to SPP. We have addressed these questions by studying the biochemical and functional properties of SPPL2b and SPPL3 in comparison to SPP. Already the analysis of their subcellular localization in cultured cells by indirect immunofluorescence, pulse-chase, and deglycosylation experiments revealed striking differences. Whereas SPPL3, like SPP, localizes to the ER, SPPL2b is predominantly found in endosomes/lysosomes. This by itself may already suggest a non-redundant function of SPPL2b. To test this hypothesis, we used the zebrafish as a model system for a functional characterization of SPP and SPPLs *in vivo*. Analysis of their expression patterns during embryogenesis and the phenotypes caused by antisense-mediated knockdown also revealed similarities between SPP and SPPL3. Both are strongly expressed in the nervous system, and their knockdown appears to cause neuronal degeneration. In contrast, SPPL2b is expressed more ubiquitously, and its knockdown results in an enlarged caudal vein without any detectable cell death. These results demonstrate that SPP and SPPLs have important functions during zebrafish embryogenesis. Moreover, they are in agreement with our cell culture data and suggest functional redundancy between SPP and SPPL3. SPPL2b, however, appears to have a role distinct from the other family members.

We then asked the question of whether the knockdown phenotypes are caused by a loss of proteolytic activity. One possibility to address this is the analysis of dominant negative mutants. For SPP, mutagenesis of the aspartate within the G*X*GD motif to alanine (D265A) has been shown to cause loss of enzymatic activity (7). We, therefore, tested the effect of the corresponding mutation in zebrafish *spp* (D268A) and found that its overexpression in zebrafish embryos results in a phenocopy of the *spp* knockdown phenotype. This suggested that active site mutations in SPP act in a dominant negative manner. Importantly, the corresponding mutations in the G*X*GD motifs of *sppl2* and *sppl3* also caused a phenocopy of the respective knockdown phenotypes, indicating that they represent active site mutations as well. These data led us to conclude that SPPL2b and SPPL3 are likely to represent active members of the SPP protease family. Moreover, we suggest that SPPL2b is an endosomal G*X*GD type aspartyl protease, which exerts a function distinct from the ER-located SPP and SPPL3.

Deficiency of the *Caenorhabditis elegans imp-2* gene, which corresponds to vertebrate SPP, also caused a severe developmental phenotype, which could be mimicked by reduced cholesterol concentrations or the disruption of *Ce-Irp-1* (48). *Ce-Irp-1* is a homologue of the vertebrate lipoprotein receptor-related protein. Interestingly, interference

with lipoprotein receptor-related proteins appears to result in neurodegeneration in mice (49), a phenotype also observed upon down-regulation of *spp* in zebrafish.

Based on the severity of the observed phenotypes, all investigated SPPLs appear to have important biological functions throughout development. This is supported by their maternal inheritance and rather ubiquitous expression. However, in the absence of specific substrates for SPPLs, one can only speculate about the physiological functions of SPPLs. The endosomal/lysosomal localization of SPPL2b suggests that it may be involved in removal of signal peptides, which escaped SPP-mediated cleavage within the ER. However, the loss-of-function phenotypes may suggest additional, more essential functions for SPPL2b. These may include generation of bioactive signaling peptides, as has been observed for SPP (7). One may even assume that intracellular cytoplasmic domains of type II transmembrane proteins may be released upon reinternalization of the substrate from the plasma membrane.

Taken together, proteolysis by G*X*GD-type aspartyl proteases within or close to the membrane indeed appears to be an "increasing scheme of variation" (24), which during evolution was fine-tuned to allow a regulated release of a variety of important signaling molecules by a number of different proteases. In addition to these essential signaling functions, some members of the SPP family may also be required to remove proteolytically generated small peptides located within the membrane of the ER or endosomes/lysosomes. A similar rather general degradation activity may also be provided by γ-secretase. However, this activity may be selective to small intramembrane stubs of type I proteins, whereas SPPs (2) and probably SPPLs as well may selectively remove proteolytically generated stubs in a type II membrane orientation.

Acknowledgments—We thank Dr. B. Martoglio and the Memorec Biotech GmbH (Cologne) for cDNAs and antibodies and S. Topp and B. Sperl for technical support.

REFERENCES

1. Brown, M. S., Ye, J., Rawson, R. B., and Goldstein, J. L. (2000) *Cell* **100,** 391–398
2. Weihofen, A., and Martoglio, B. (2003) *Trends Cell Biol.* **13,** 71–78
3. Urban, S., Lee, J. R., and Freeman, M. (2001) *Cell* **107,** 173–182
4. Lee, J. R., Urban, S., Garvey, C. F., and Freeman, M. (2001) *Cell* **107,** 161–171
5. Wolfe, M. S., Xia, W., Ostaszewski, B. L., Diehl, T. S., Kimberly, W. T., and Selkoe, D. J. (1999) *Nature* **398,** 513–517
6. Weihofen, A., Lemberg, M. K., Ploegh, H. L., Bogyo, M., and Martoglio, B. (2000) *J. Biol. Chem.* **275,** 30951–30956
7. Weihofen, A., Binns, K., Lemberg, M. K., Ashman, K., and Martoglio, B. (2002) *Science* **296,** 2215–2218
8. Selkoe, D., and Kopan, R. (2003) *Annu. Rev. Neurosci.* **26,** 565–597
9. Haass, C., and Steiner, H. (2002) *Trends Cell Biol.* **12,** 556–562
10. Haass, C. (2004) *EMBO J.* **23,** 483–488
11. Edbauer, D., Winkler, E., Regula, J. T., Pesold, B., Steiner, H., and Haass, C. (2003) *Nat. Cell. Biol.* **5,** 486–488
12. Takasugi, N., Tomita, T., Hayashi, I., Tsuruoka, M., Niimura, M., Takahashi, Y., Thinakaran, G., and Iwatsubo, T. (2003) *Nature* **422,** 438–441
13. Kimberly, W. T., LaVoie, M. J., Ostaszewski, B. L., Ye, W., Wolfe, M. S., and Selkoe, D. J. (2003) *Proc. Natl. Acad. Sci. U. S. A.* **100,** 6382–6387
14. Kim, S. H., and Sisodia, S. S. (2005) *J. Biol. Chem.* **280,** 1992–2001
15. Steiner, H., Duff, K., Capell, A., Romig, H., Grim, M. G., Lincoln, S., Hardy, J., Yu, X., Picciano, M., Fechteler, K., Citron, M., Kopan, R., Pesold, B., Keck, S., Baader, M., Tomita, T., Iwatsubo, T., Baumeister, R., and Haass, C. (1999) *J. Biol. Chem.* **274,** 28669–28673
16. Zhang, Z., Nadeau, P., Song, W., Donoviel, D., Yuan, M., Bernstein, A., and Yankner, B. A. (2000) *Nat. Cell. Biol.* **2,** 463–465
17. Herreman, A., Serneels, L., Annaert, W., Collen, D., Schoonjans, L., and De Strooper, B. (2000) *Nat. Cell. Biol.* **2,** 461–462
18. De Strooper, B. (2003) *Neuron* **38,** 9–12
19. Shirotani, K., Edbauer, D., Prokop, S., Haass, C., and Steiner, H. (2004) *J. Biol. Chem.* **279**, 41340–41345
20. Ma, G., Li, T., Price, D. L., and Wong, P. C. (2005) *J. Neurosci.* **25,** 192–198
21. Serneels, L., Dejaegere, T., Craessaerts, K., Horre, K., Jorissen, E., Tousseyn, T., Hebert, S., Coolen, M., Martens, G., Zwijsen, A., Annaert, W., Hartmann, D., and De Strooper, B. (2005) *Proc. Natl. Acad. Sci. U. S. A.* **102,** 1719–1724
22. Steiner, H., Kostka, M., Romig, H., Basset, G., Pesold, B., Hardy, J., Capell, A., Meyn, L., Grim, M. G., Baumeister, R., Fechteler, K., and Haass, C. (2000) *Nat. Cell. Biol.* **2,** 848–851
23. Martoglio, B., and Golde, T. E. (2003) *Hum. Mol. Genet.* **12,** 201–206
24. Wolfe, M. S., and Kopan, R. (2004) *Science* **305,** 1119–1123
25. LaPointe, C. F., and Taylor, R. K. (2000) *J. Biol. Chem.* **275,** 1502–1510
26. Kimberly, W. T., Xia, W., Rahmati, T., Wolfe, M. S., and Selkoe, D. J. (2000) *J. Biol. Chem.* **275,** 3173–3178
27. Weihofen, A., Lemberg, M. K., Friedmann, E., Rueeger, H., Schmitz, A., Paganetti, P., Rovelli, G., and Martoglio, B. (2003) *J. Biol. Chem.* **278,** 16528–16533
28. Nyborg, A. C., Kornilova, A. Y., Jansen, K., Ladd, T. B., Wolfe, M. S., and Golde, T. E. (2004) *J. Biol. Chem.* **279,** 15153–15160
29. Kornilova, A. Y., Das, C., and Wolfe, M. S. (2003) *J. Biol. Chem.* **278,** 16470–16473
30. Ponting, C. P., Hutton, M., Nyborg, A., Baker, M., Jansen, K., and Golde, T. E. (2002) *Hum. Mol. Genet.* **11,** 1037–1044
31. Grigorenko, A. P., Moliaka, Y. K., Korovaitseva, G. I., and Rogaev, E. I. (2002) *Biochemistry* (*Mosc*) **67,** 826–835
32. Citron, M., Oltersdorf, T., Haass, C., McConlogue, L., Hung, A. Y., Seubert, P., Vigo-Pelfrey, C., Lieberburg, I., and Selkoe, D. J. (1992) *Nature* **360,** 672–674
33. Haass, C., Schlossmacher, M. G., Hung, A. Y., Vigo-Pelfrey, C., Mellon, A., Ostaszewski, B. L., Lieberburg, I., Koo, E. H., Schenk, D., Teplow, D. B., and Selkoe, D. J. (1992) *Nature* **359,** 322–325
34. Fluhrer, R., Capell, A., Westmeyer, G., Willem, M., Hartung, B., Condron, M. M., Teplow, D. B., Haass, C., and Walter, J. (2002) *J. Neurochem.* **81,** 1011–1020
35. Mullins, M. C., Hammerschmidt, M., Haffter, P., and Nusslein-Volhard, C. (1994) *Curr. Biol.* **4,** 189–202
36. Kimmel, C. B., Ballard, W. W., Kimmel, S. R., Ullmann, B., and Schilling, T. F. (1995) *Dev. Dyn.* **203,** 253–310
37. Schulte-Merker, S., Ho, R. K., Herrmann, B. G., and Nusslein-Volhard, C. (1992) *Development* **116,** 1021–1032
38. Friedmann, E., Lemberg, M. K., Weihofen, A., Dev, K. K., Dengler, U., Rovelli, G., and Martoglio, B. (2004) *J. Biol. Chem.* **279,** 50790–50798
39. Edbauer, D., Winkler, E., Haass, C., and Steiner, H. (2002) *Proc. Natl. Acad. Sci. U. S. A.* **99,** 8666–8671
40. Herreman, A., Van Gassen, G., Bentahir, M., Nyabi, O., Craessaerts, K., Mueller, U., Annaert, W., and De Strooper, B. (2003) *J. Cell Sci.* **116,** 1127–1136
41. Leem, J. Y., Vijayan, S., Han, P., Cai, D., Machura, M., Lopes, K. O., Veselits, M. L., Xu, H., and Thinakaran, G. (2002) *J. Biol. Chem.* **277,** 19236–19240
42. Martoglio, B., and Dobberstein, B. (1998) *Trends Cell Biol.* **8,** 410–415
43. Chen, J. W., Murphy, T. L., Willingham, M. C., Pastan, I., and August, J. T. (1985) *J. Cell Biol.* **101,** 85–95
44. Leimer, U., Lun, K., Romig, H., Walter, J., Grunberg, J., Brand, M., and Haass, C. (1999) *Biochemistry* **38,** 13602–13609
45. Geling, A., Steiner, H., Willem, M., Bally-Cuif, L., and Haass, C. (2002) *EMBO Rep.* **3,** 688–694
46. Haffner, C., Frauli, M., Topp, S., Irmler, M., Hofmann, K., Regula, J. T., Bally-Cuif, L., and Haass, C. (2004) *EMBO J.* **23,** 3041–3050
47. Furutani-Seiki, M., Jiang, Y. J., Brand, M., Heisenberg, C. P., Houart, C., Beuchle, D., van Eeden, F. J., Granato, M., Haffter, P., Hammerschmidt, M., Kane, D. A., Kelsh, R. N., Mullins, M. C., Odenthal, J., and Nusslein-Volhard, C. (1996) *Development* **123,** 229–239
48. Grigorenko, A. P., Moliaka, Y. K., Soto, M. C., Mello, C. C., and Rogaev, E. I. (2004) *Proc. Natl. Acad. Sci. U. S. A.* **101,** 14955–14960
49. Van Uden, E., Mallory, M., Veinbergs, I., Alford, M., Rockenstein, E., and Masliah, E. (2002) *J. Neurosci.* **22,** 9298–9304

Differential Localization and Identification of a Critical Aspartate Suggest Non-redundant Proteolytic Functions of the Presenilin Homologues SPPL2b and SPPL3

Peter Krawitz, Christof Haffner, Regina Fluhrer, Harald Steiner, Bettina Schmid and Christian Haass

J. Biol. Chem. 2005, 280:39515-39523.
doi: 10.1074/jbc.M501645200 originally published online July 5, 2005
